WATER RESOURCES RESEARCH, VOL. 34, NO. 8, PAGES 1971–1985, AUGUST 1998

Parameterization of stream channel geometry in the distributed modeling of catchment dynamics

Stefano Orlandini

Dipartimento di Ingegneria delle Strutture, dei Trasporti, delle Acque, del Rilevamento, del Territorio, Università degli Studi di Bologna, Bologna, Italy

Renzo Rosso

Dipartimento di Ingegneria Idraulica, Ambientale e del Rilevamento, Politecnico di Milano, Milan, Italy

Abstract. A simple and efficient procedure for incorporating the effects of stream channel geometry in the distributed modeling of catchment dynamics is developed. At-a-station and downstream fluvial relationships are combined and the obtained laws of variability in space and time for water-surface width and wetted perimeter are incorporated into a diffusion wave routing model based on the Muskingum-Cunge method with variable parameters. The parameterization obtained is applied to the approximately 840-km^2 Sieve catchment (Central Italian Apennines) to test the possibility of estimating channel geometry parameters from cross-section surveys and to assess the impact of dynamic variations in the channel geometry on catchment dynamics. The use of the estimated channel geometry in surface runoff routing produces a significant improvement in the flood hydrograph description at the catchment outlet with respect to less detailed network parameterizations. In addition, the results obtained from a "downstream" analysis of the velocity field indicate that the stream characteristics related to the locally varying cross-section shape may have a strong control on flow velocities, and thus they should be monitored and synthesized for a comprehensive description of the distributed catchment dynamics.

1. Introduction

Recent advances in remote sensing, geographic information systems, and computer technology make the use of distributed hydrologic models an attractive approach to flow simulation and prediction. The linkage of a distributed hydrologic model with the spatial data handling capabilities of digital elevation models (DEMs) and digital terrain models (DTMs) offers advantages associated with utilizing the full information content of spatially distributed data to analyze hydrologic processes. The major areas of application of distributed models are in forecasting the effects of land use change, the effects of spatially variable inputs and outputs, the movement of pollutants and sediments, and the hydrologic response of ungauged catchments [*Beven and O'Connell*, 1982].

Surface runoff constitutes an important component of the hydrologic response of a catchment to climate and land use forcing. The early work by *Sherman* [1932] has influenced the approach taken by many engineers and scientists in characterizing components of hydrographs and in methods for estimating catchment response to a given storm. However, a description of hydrologic response using either a unit hydrograph (UH) or instantaneous unit hydrograph (IUH) assumes a time invariant and linear response [*Dooge*, 1959]. This is not always realistic, especially for small catchments [*Minshall*, 1960]. A pioneering approach to physical modeling of surface runoff was initiated through the simplified model of a catchment idealized by an open book geometry [*Wooding*, 1965a, b, 1966].

Paper number 98WR00257.
0043-1397/98/98WR-00257$09.00

Wooding [1965b] demonstrated that the nonlinearity inherent in his descriptions of hillslopes and network responses results in a catchment's unit response departing from linear theory such that peak discharge is not linearly proportional to the rainfall excess intensity, and the time to peak is not constant. *Wooding*'s [1965b] analysis did not examine the effects of complex stream network geometry upon catchment responses. A variety of methods exists for automatically extracting channel network from DEMs [e.g., *Mark*, 1983; *Band*, 1986; *Morris and Heerdegen*, 1988; *Smith et al.*, 1990; *Montgomery and Foufoula-Georgiou*, 1993], but little attention has been paid to the role of the stream channel geometry in hydrologic routing [e.g., *Howard*, 1990; *Myers*, 1991]. The control of channel geometry on velocity and travel times determines the distribution of flood storage over the watershed. In some of the traditional hydrograph synthesis procedures, this distribution of storage is represented by a conceptual model of storage elements, through which the rainfall excess and runoff are routed. Determination of sizes and arrangement of the storage elements in the computational model are usually carried out by relating velocities or storage to some geomorphological parameters (which are usually a function of stream length and channel slope) or by performing hydraulic calculations to estimate velocity in various reaches of the stream system of the watershed. In both cases, numerical constants are normally determined by fitting computed hydrographs to observed ones. However, this approach may neglect the storage and travel time in the small tributary channels and in overland flow, and generally inadequate data are available, particularly for the high flood flows of interest. In addition, cross-sectional area, hydraulic radius, and slope often vary markedly within reaches of natural streams,

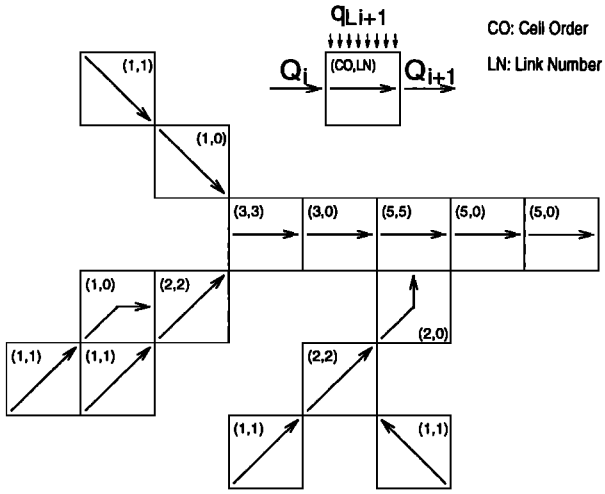

Figure 1. Sketch of the DEM-based drainage network ordering system introduced in section 2.1.

and average values may not be representative. In the present paper a new method for incorporating the effects of dynamic variations in channel geometry in a distributed, DEM-based flood-routing model is developed. The method is tested on the Sieve catchment of the Central Italian Apennines.

2. Model Formulation

The catchment hydrologic response is considered as if determined by the two processes of hillslope and channel transport, operating across all the hillslopes and stream channels forming a catchment. The developed formulation is designed to improve the description of surface runoff propagation in a generic drainage system, where both infiltration-excess (Horton type) and saturation-excess (Dunne type) surface runoff production mechanisms occur. Surface runoff is not allowed to infiltrate in downslope cells even when the soil profile of these cells is not saturated. The runoff-runon problem is likely to be important where broad sheet flow occurs but relatively unimportant when the flow concentrates in defined rills, channels, and streams, as assumed here. There are two main aspects of the catchment model presented in this work. The first aspect concerns the description of a natural drainage system in terms of hydrologically relevant features; the second concerns the incorporation of these features into a distributed, diffusion wave model of catchment dynamics.

2.1. Drainage System Description

Surface runoff over hillslopes or agricultural watersheds initially starts as sheet flow, then it concentrates into a series of small channels. The flow concentrations are due to either topographic irregularities or differences in soil erodibility. As runoff continues, erosion progresses and these channels deepen and widen as a function of slope steepness, runoff characteristics, and soil erodibility. Such erosion-formed microchannels are called rills or rivulets [*Emmett*, 1978; *Li et al.*, 1980]. At the hillslope base runoff is drained by the stream network. The propagation of flow in space and time through a mountain network of rills and streams is mainly complicated by three factors: junctions and tributaries, variation in cross section, and variation in resistance as a function both of flow depth and of location along the stream channel.

In the proposed formulation the drainage system topography and composition are described by extracting automatically a conceptual drainage network from the catchment DEM. Each of the DEM cells is characterized by a maximum-slope pointer, and the conceptual channels within cells are organized into the ordering system sketched in Figure 1. Ordering is defined by assigning to each cell two numbers: the cell order and the link number. The first is the sum of the orders of the neighboring upslope cells from which the cell can receive water; source cells are assigned order 1. The link number identifies the first cell of each link in the drainage system; it is equal to the cell order for the uppermost cell of the link and to zero for the other link cells. Distinction between hillslope rill and network channel cells is based on the "constant critical support area concept" as described by *Montgomery and Foufoula-Georgiou* [1993]. Rill flow is assumed to occur for all those catchment cells for which the upstream drainage area A does not exceed the constant threshold value A_*, while channel flow is assumed to occur for all those cells for which A equals or exceeds A_*. More sophisticated criteria for identifying hillslopes and channels, such as that of "critical value of normalized convergence" introduced by *Howard* [1994], may be used in those cases for which the simple "constant critical support area concept" provides unsatisfactory outcomes. While an explicit description of network composition and locally varying channel bed slope can be obtained by purely processing the catchment DEM, additional concepts are required to incorporate the effects of locally varying channel geometry and roughness on flow propagation. In the proposed formulation attention is focused on both at-a-station and downstream variabilities in channel network geometry, whereas channel roughness is assumed to vary in a downstream direction along the drainage system but not at a given station. In this regard the detail with which the natural system is described is forfeited in exchange for simplicity to better identify the effects of the innovative aspects in the proposed formulation.

If surveying of the cross-sectional geometries of one-dimensional river systems is normally an exacting but possible task, an adequate field inspection of natural drainage systems may require prohibitive efforts, especially for catchments of practical interest. In addition, since mountain rivers construct their own geometries, the stream channel geometry of natural drainage systems is often subjected to radical change, and this would require a continuous updating of surveys. In the impossibility of direct acquirement of channel geometry for complex drainage systems, a conceptual representation of the broad features of channel geometry may be formulated on the basis of fluvial geomorphological studies pioneered, among others, by *Kennedy* [1895], *Lacey* [1929], and *Blench* [1951] for stable canals and by *Leopold and Maddock* [1953] and *Lane* [1957] for rivers. The studies of *Leopold and Maddock* [1953] showed that superimposed on the great heterogeneity among any group of stream channels there were certain broad generalizations that tied natural river channels into continua, on which certain characteristics seemed to apply equally to a wide variety of cases. Described under the term "hydraulic geometry," these generalizations indicated that in responding to loads of water and sediment imposed on them, rivers changed their forms in discernible ways. Fluvial geomorphological relationships provide insights on the variation of hydraulic geometry of reaches within a channel system and this may synthesize the information required for a particular drainage system in order to describe the effects of the dynamic variations in channel geom-

etry on catchment dynamics. In the proposed parameterization fluvial relationships are used to characterize both hillslope rills and network channels dynamics. The extension of power law hydraulic geometry derived for rivers to hillslope rills is carried out in the present work heuristically, and future experimental and theoretical efforts may be devoted to providing an exhaustive validation of this model assumption.

The relevant channel geometry in the diffusion wave modeling of catchment dynamics is synthesized by combining at-a-station and downstream fluvial relationships for water-surface width and wetted perimeter. According to *Leopold and Maddock* [1953], if one considers discharge of various frequencies, Q, at a point of the river network, the water-surface width W scales with Q as

$$W = a' Q^{b'}, \tag{1}$$

where the scaling coefficient a' depends on the location of that point and the exponent b' is a characteristic of the channel network as a whole. When considering discharge with the same frequency, Q_r, at different points moving downstream in the basin, the corresponding channel width W_r is given by

$$W_r = a'' Q_r^{b''}, \tag{2}$$

where a'' and b'' are characteristics of the river network. Although this is not necessarily equivalent to considering discharge resulting from the same event at different points, it can be assumed as a reasonable indicator of what may occur in that situation [*Bras*, 1990].

Relationships (1) and (2) are combined into a single equation to represent the dynamics of water-surface flow width at any point of the channel network in response to surface runoff forcing events. From equation (1) one obtains, for a given point in the channel network,

$$\frac{W}{W_r} = \left(\frac{Q}{Q_r}\right)^{b'}, \tag{3}$$

where W_r and Q_r are the values of flow width and discharge at that point as given by (2). Equation (2) yields

$$\frac{W_r}{W_{ro}} = \left(\frac{Q_r}{Q_{ro}}\right)^{b''}, \tag{4}$$

where W_{ro} and Q_{ro} are the values of the flow width and discharge at the basin outlet, for the considered frequency. By combining (3) and (4), one obtains

$$W = W_{ro}\left(\frac{Q_r}{Q_{ro}}\right)^{b''}\left(\frac{Q}{Q_r}\right)^{b'}. \tag{5}$$

As discharges in the various reaches corresponding to an outflow Q_{ro} are not known, estimation from a geomorphological relation is necessary. *Leopold et al.* [1964] report a relation of wide applicability as

$$Q_b \propto A^{0.75}, \tag{6}$$

where Q_b is the bank-full discharge and A is the drainage area. The observed exponent in (6) arises from two important factors: nonuniform precipitation and the diffusional effects of downstream flow routing (A. D. Howard, personal communication, 1997). Since the routing model will account for the latter and since spatially explicit modeling of precipitation could account for the former, in the proposed formulation the exponent in (6) is assumed equal to unity. Under this assumption and using Q_b for Q_r, it is assumed that $Q_r \propto A$ and thus

$$\frac{Q_r}{Q_{ro}} = \frac{A}{A_o}, \tag{7}$$

A_o being the catchment area, which is substituted for Q_r/Q_{ro} in (5) to obtain

$$W = \mathcal{W} Q^{b'}, \tag{8}$$

where $\mathcal{W}$ is a variable scaling coefficient depending on location in the river network and is given by

$$\mathcal{W} = W_{ro} Q_{ro}^{-b'} (A/A_o)^{b''-b'}, \tag{9}$$

W_{ro} being the water surface width at the catchment outlet corresponding to the arbitrary but fixed value of flow discharge Q_{ro}.

Lacey [1939] utilized measurements of channel characteristics made on reaches of Indian canals that through time had achieved a stable cross section. He proposed a number of empirical equations that were derived from these data. Included in his "basic equations" is one relating wetted perimeter P to discharge Q. This equation is identical in form to the downstream width-discharge relationship found by *Leopold and Maddock* [1953] for river data, inasmuch as the wetted perimeter P is nearly equal to the water-surface width W as it verifies for wide channels. *Lacey* [1939] recognized that his equation relating wetted perimeter to discharge applied to many natural streams, but having few river data, he could not explore the limits of its applicability. Because of the small range of intercepts in the canal data and the fact that the few individual measurements on rivers also happened to plot with nearly the same intercept as the canal data, *Lacey* [1939] concluded that his fluvial relationship was fundamental and that it was independent of sediment size. Following *Lacey* [1939], the at-a-station fluvial relationship for the wetted perimeter can be written as

$$P = c' Q^{d'}, \tag{10}$$

where the scaling coefficient c' depends on the section location and the exponent d' is a characteristic of the channel network as a whole. When considering discharge with the same frequency, Q_r, at different points moving downstream in the basin, the corresponding channel width P_r is given by

$$P_r = c'' Q_r^{d''}, \tag{11}$$

where c'' and d'' are characteristics of the river network. Relationships (10) and (11) are combined into a single equation to represent the dynamics of wetted perimeter at any point of the channel network in response to surface runoff forcing events, yielding

$$P = \mathcal{P} Q^{d'}, \tag{12}$$

where $\mathcal{P}$ is a variable scaling coefficient depending on location in the river network and is given by

$$\mathcal{P} = P_{ro} Q_{ro}^{-d'} (A/A_o)^{d''-d'}, \tag{13}$$

P_{ro} being the wetted perimeter at the catchment outlet corresponding to the arbitrary but fixed value of flow discharge Q_{ro}.

An additional relationship concerns the cross-sectional flow area Ω. From the at-a-station and downstream relationships

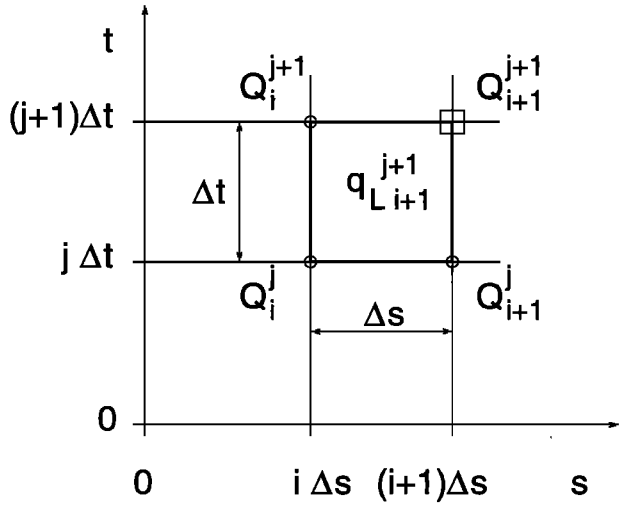

Figure 2. Space-time computational grid of the Muskingum-Cunge method.

$$\Omega = e' Q^{f'} \tag{14}$$

$$\Omega = e'' Q^{f''}, \tag{15}$$

where the scaling coefficient e' depends on the location of the considered cross section, while f', e'', and f'' are characteristics of the river network, one can obtain

$$\Omega = \Omega_{r\,o} Q_{r\,o}^{-f'} (A/A_o)^{f''-f'} Q^{f'}, \tag{16}$$

$\Omega_{r\,o}$ being the cross-sectional flow area at the catchment outlet corresponding to the arbitrary but fixed value of flow discharge $Q_{r\,o}$. The parameters $(\Omega_{r\,o}, f', f'')$ will be estimated in section 3.1 on the basis of the hydraulic laws of flow resistance, and the obtained relationship will be used at the end of section 3.2 to synthesize the variability in space and time of Ω during flood events. Relationship (16) will not be incorporated into the routing scheme developed in section 2.2.

The relevant hydraulic geometry in natural drainage systems is synthesized through (8), (9), (12), and (13), where, once $Q_{r\,o}$ is fixed, $(W_{r\,o}, b', b'')$ and $(P_{r\,o}, d', d'')$ are the only structural parameters of the system. Field inspection is required to provide estimates of these structural parameters for both hillslope rill and network channel geometries in a given drainage system. During a flood the active channel water-surface width and wetted perimeter scale dynamically with discharge with the same exponent of the at-a-station relationships, and with the upstream basin area with an exponent equal to the difference of those of downstream and at-a-station relationships. The effects of the dynamic variations in rill and channel geometry on flow propagation are reproduced by incorporating (8), (9), (12), and (13) into a distributed, DEM-based flood-routing model.

2.2. Diffusion Wave Modeling

A routing scheme developed on the basis of the Muskingum-Cunge method with variable parameters is used in the present study to describe both hillslope rill and network channel flows. This scheme is based on the formulation introduced by *Cunge* [1969] and further extended by *Ponce and Yevjevich* [1978] and *Ponce* [1986]. The model routes surface runoff downstream from the uppermost DEM cell in the basin to the outlet, following the drainage network ordering system described in section 2.1 (Figure 1). A given cell will receive water from its upslope neighbors and discharge to its downslope neighbor. For cells of flow convergence the upstream inflow hydrograph is taken as the sum of the outflow hydrographs of the neighboring upslope cells from which the cell receives water. At any catchment cell the lateral inflow rate (discharge per unit channel length) to the elemental channel within the cell is given by

$$q_L = q \Delta x \Delta y / \Delta s, \tag{17}$$

where q denotes the local contribution rate (discharge per unit catchment area) to surface runoff, Δx and Δy are the cell spacings in the direction of the x and y horizontal coordinates, and Δs is the channel length within the cell. Inflow hydrographs and lateral inflows q_L are routed onto each elemental channel via the routing equation

$$Q_{i+1}^{j+1} = C_1 Q_i^{j+1} + C_2 Q_i^j + C_3 Q_{i+1}^j + C_4 q_{Li+1}^{j+1}, \tag{18}$$

where Q_{i+1}^{j+1} is the discharge at network link point $(i + 1)\Delta s$ and time $(j + 1)\Delta t$, and q_{Li+1}^{j+1} is the lateral inflow rate at the $(i + 1)$th link cell and $(j + 1)$th time interval (Figure 2). The routing coefficients, C_1, C_2, C_3, and C_4, are expressed by the *Natural Environment Research Council* [1975] as

$$C_1 = \frac{c_k(\Delta t/\Delta s) - 2X}{2(1 - X) + c_k(\Delta t/\Delta s)}, \tag{19}$$

$$C_2 = \frac{c_k(\Delta t/\Delta s) + 2X}{2(1 - X) + c_k(\Delta t/\Delta s)}, \tag{20}$$

$$C_3 = \frac{2(1 - X) - c_k(\Delta t/\Delta s)}{2(1 - X) + c_k(\Delta t/\Delta s)}, \tag{21}$$

$$C_4 = \frac{2c_k \Delta t}{2(1 - X) + c_k(\Delta t/\Delta s)}, \tag{22}$$

where c_k is the kinematic wave celerity and X is the weighting factor introduced by *Cunge* [1969] for discretizing the kinematic flow equation

$$\frac{\partial Q}{\partial t} + c_k \frac{\partial Q}{\partial s} = c_k q_L. \tag{23}$$

This weighting factor X is used to match the numerical diffusion coefficient of the scheme

$$D_n = c_k \Delta s (1/2 - X), \tag{24}$$

and the hydraulic diffusivity D_h in the convection-diffusion flow equation

$$\frac{\partial Q}{\partial t} + c_k \frac{\partial Q}{\partial s} = D_h \frac{\partial^2 Q}{\partial s^2} + c_k q_L. \tag{25}$$

Incorporating (12) into the Manning-Gauckler-Strickler friction equation

$$Q = k_S S_f^{1/2} P(Q)^{-2/3} \Omega^{5/3}, \tag{26}$$

where k_S is the apparent Gauckler-Strickler roughness coefficient ($k_S = 1/n$, n being the Manning roughness coefficient), S_f is the friction slope (slope of the energy grade line), Ω is the flow area, and the wetted perimeter P is expressed as a function of Q on the basis of the kinematic flow assumption (that implies a single stage flow rating curve), yields

$$Q = k_S^{3/(3+2d')} S_f^{3/[2(3+2d')]} \mathcal{P}^{-2/(3+2d')} \Omega^{5/(3+2d')}. \tag{27}$$

As shown in the appendix, the kinematic flood wave celerity $c_k = dQ/d\Omega$ is

$$c_k = 5/(3 + 2d')k_S^{3/5}S_o^{3/10}\mathcal{P}^{-2/5}Q^{2/5(1-d')}, \quad (28)$$

where $S_o = \sin\beta$ is the channel bed slope, β being the channel bed inclination angle. On the basis of (8) and (12) the hydraulic diffusivity D_h is expressed by

$$D_h = \frac{3Q^{1-b'}\cos\beta}{2(3 + 2d')\mathcal{W}S_o}, \quad (29)$$

and thus, by matching D_n and D_h given by (24) and (29), respectively, the weighting factor X can be expressed as a function of channel and flow characteristics, that is

$$X = 1/2(1 - D), \quad (30)$$

where D is the cell Reynolds number,

$$D = \frac{3Q^{1-b'}\cos\beta}{(3 + 2d')\mathcal{W}S_o c_k \Delta s}. \quad (31)$$

Wave celerity c_k and weighting factor X are varied at each computational cell according to (28), (30), and (31), in which discharge Q is estimated via a three-point average discharge $\bar{Q} = (Q_i^j + Q_{i+1}^j + Q_i^{j+1})/3$ [*Ponce and Yevjevich*, 1978]. By varying X with flow the numerical diffusion coefficient D_n is used to simulate the hydraulic diffusivity D_h of the actual flood wave. For $X = 1/2$ there is no numerical diffusion. For $X > 1/2$ the numerical diffusion coefficient is negative, and the numerical scheme is therefore unstable; however, such occurrence is avoided by matching numerical and physical diffusivities, and this ensures the unconditional stability of the scheme. In the Muskingum-Cunge method X is interpreted as a diffusion-matching factor, and thus negative values of X are possible. The reliability and robustness of the developed scheme in terms of mass conservation, accuracy, and consistency (referred to by *Ponce* [1986] as the ability of the routing procedure to produce the same results regardless of grid size) are discussed by *Orlandini and Rosso* [1996]. Advantages of the Muskingum-Cunge method with variable parameters over the standard kinematic wave methods are discussed by *Ponce* [1986]. Some of the disadvantages of the Muskingum-Cunge method are that it cannot handle downstream disturbances that propagate upstream and that it does not accurately predict the discharge hydrograph at a downstream boundary when there are large variations in the kinematic wave speed such as those that result from inundation of large flood plains [*Natural Environment Research Council*, 1975]. Simulation of backwater effects in catchment dynamics can be relevant to allow flow over "digital dams" (due to errors in DEM data). For example, in the model presented by *Julien et al.* [1995], surface water accumulates behind the barrier until the depth exceeds the barrier height and then spills over. In the formulation presented here, "digital pits" are filled in a preprocessing step, before extracting the channel network from the catchment DEM, so that a certain degree of accuracy in the catchment topography representation is forfeited in exchange for simplicity and robustness in the flow dynamics description. It is emphasized here that fluvial relationships for water-surface width W and wetted perimeter P are incorporated into the routing model to improve the description of catchment dynamics expressed in terms of flow discharge Q. The dynamic variations of mean flow depth $Y_m = \Omega/W$, hydraulic radius $R = \Omega/P$, and mean flow velocity $U = Q/\Omega$ can be obtained from the calculated values of Q on the basis of the kinematic flow assumption expressed by (27) and using the relationships (8), (9), (12), and (13).

3. Catchment Application

The developed parameterization is applied to the Sieve catchment, located in the Central Italian Apennines, near the city of Florence. The area of the Sieve catchment is $A_o = 841.76$ km^2. Except in the valley, which is dedicated to agriculture, the terrain is forested and mountainous, with an average elevation of 470 m above sea level. The elevation of the highest peak is 1657 m, and the outlet is at 50 m above sea level. The climate is Mediterranean. The rainy season lasts from October until April, with peaks in November and February. Runoff generation is mostly infiltration excess (Horton type) overland flow, a consequence of heavy storms over steeply sloping terrains with low hydraulic conductivities ($\sim 10^{-1}$–10^0 mm h^{-1}). Under these particular circumstances the model developed by *Orlandini et al.* [1996] is used to describe water yield from hillslopes. This model consists of a time compression approximation (TCA) soil water balance model, which provides local contributions to surface and subsurface runoff at each DEM cell and for each time step of the discretized simulation period. Surface and subsurface runoff are routed downstream by means of two different diffusion wave schemes based on the Manning-Gauckler-Strickler and Darcy flow equations, respectively. At the hillslope base subsurface runoff is drained by the channel network and it is routed (along with surface runoff) towards the catchment outlet. It is stressed here that the parameterization developed in the present paper is aimed at improving the description of the surface runoff propagation process, independently of the production mechanisms from which this surface runoff is generated.

The catchment area is horizontally discretized into 5261 cells with a 400-m grid spacing (Figure 3). The DEM is processed to obtain estimated distributed terrain slopes and the automatically generated drainage network described in section 2.1. Hillslope rill and network channel cells are identified through the "critical support area concept" with constant threshold $A_* = 1.28$ km^2, corresponding to eight DEM cells. This threshold area produces a network that compares very favorably with blue lines depicted in topographic maps at the scale 1:200,000 [*Carlá et al.*, 1987]. Surface cover and soil properties are assigned to each DEM cell, and the TCA water balance model developed by *Orlandini et al.* [1996] is applied to calculate local contribution to infiltration excess runoff in response to storm events at 1-hour time step resolution. Gauckler-Strickler roughness is also assigned to each DEM cell of the catchment on the basis of data reported in the literature [e.g., *Emmett*, 1978; *Bathurst*, 1993]. In order to explore the hydraulic implications of the locally varying channel shape in the Sieve drainage system, the surveyed features of many cross sections along the catchment mainstream are synthesized to provide estimates of the channel geometry structural parameters introduced in section 2.1, and surface runoff is routed using the model developed in section 2.2.

3.1. Estimating Channel Geometry Parameters

Downstream scaling coefficients and exponents reported in published hydraulic geometry relationships exhibit considerable variation [*Park*, 1977]. Reported values of the downstream

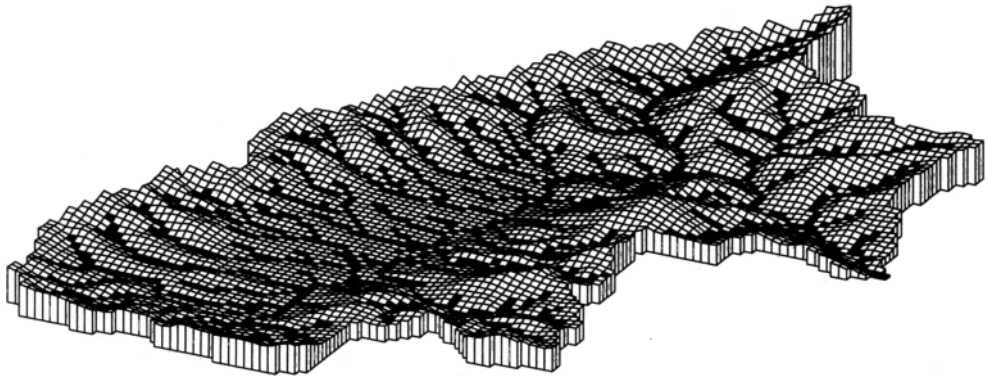

Figure 3. A 400 m × 400 m resolution Sieve catchment DEM showing the cells in which hillslope rill flow (white cells) and network channel flow (black cells) occurs.

width exponent b'' in (2), for instance, range from 0.20 to 0.65, with an average value of 0.50 [*Carlston*, 1969; *Knighton*, 1987]. Downstream scaling coefficients are generally more variable than exponents [*Knighton*, 1987]. Hence the estimation of scaling coefficients and exponents of the relevant hydraulic geometry of natural drainage systems should be based on detailed field inspections, where simultaneous measurements of both geometry and flow characteristics are carried out [e.g., *Osterkamp and Hedman*, 1977; *Mosley*, 1981; *Rhoads*, 1991; *Kolberg and Howard*, 1995]. However, costs and time required for such inspections make them not always justified for many applications in river engineering. In those circumstances a procedure of parameterization based on the surveying of only the cross-sectional shapes may be a useful tool for incorporating the broad features of channel geometry in hydrologic routing. This problem is dealt with in the present section with reference to the Sieve catchment.

For the Sieve catchment, only a detailed survey of 144 cross sections along the mainstream is available. This information is assumed to be adequate to characterize the network channel geometry, whereas reasonable but not field-based parameter evaluations are used to characterize hillslope rill geometry, assuming that the response of hillslopes is relatively less important than network response for the considered drainage system. As shown by *Wooding* [1965b], *Kirkby* [1976], and *Beven and Wood* [1993], for small catchments ($A < 100$ km^2) hillslope response is more important than network response; with increasing catchment size, catchment response becomes increasingly dominated by the network response. Channel geometry parameters introduced in section 2.1 are calibrated through a DEM-based automatic procedure that can consider only a single cross-section survey for each DEM cell. For this reason only 87 of the 144 available cross-section surveys along the Sieve catchment main channel are used in the following calibration exercise. Two of these channel surveys are shown as examples in Figure 4.

For each surveyed cross section, local channel roughness and slope are extracted from DTM and DEM data so that flow characteristics $W = W(Q)$, $P = P(Q)$, and $\Omega = \Omega(Q)$ are calculated on the basis of the Manning-Gauckler-Strickler uniform flow equation. Since the considered cross sections display compound shapes (as generally happens in nature), following common practice they are divided into several distinct subsections (vertical slices) and, to take account of the different flow velocities in the various subsections, the uniform flow equation (26) is expressed in the form

$$Q = k_S S_o^{1/2} \sum_{i=1}^{N_p} P_i^{-2/3} \Omega_i^{5/3}, \tag{32}$$

where the roughness coefficient k_S ($k_S = 1/n$, n being the Manning roughness) and the local channel bed slope S_o are assumed to be constant over the N_p slices into which the section is subdivided, whereas P_i and Ω_i are the wetted perimeter and flow area of the ith slice ($i = 1, \cdots, N_p$), respectively. The calculated characteristics for W, P, and Ω are obtained by means of (32), generating for increasing flow depths in the section an adequate number of data points (Q, W), (Q, P), and (Q, Ω), respectively. The calculated data

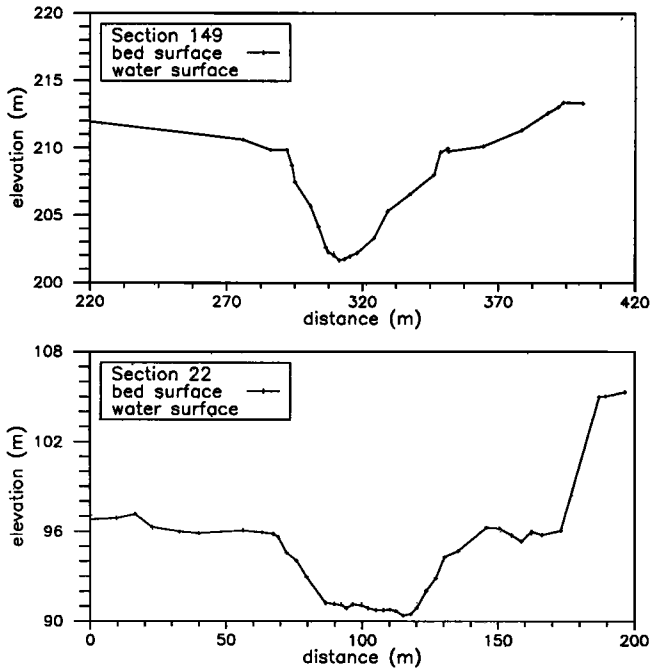

Figure 4. Two surveyed cross sections of the upper (section 149) and lower (section 22) part of the main stream in the Sieve catchment (Figure 9, Table 4). Dots indicate the water-surface level at the time of surveying.

points are used as standards and fitted to the power function models given by (1), (10), and (14), respectively, so that estimates of the at-a-station scaling coefficients and exponents (a', b'), (c', d'), and (e', f'), respectively, are provided. Logarithms are introduced to solve fitting problems as ordinary least squares (OLS) linear regressions and coefficients of determination r^2 are calculated to provide a goodness-of-fit measure. This procedure is shown for water-surface width in Figure 5 (where linear scales are used), with reference to the two cross sections of Figure 4. The calculated characteristics $W = W(Q)$ are given by an adequate number of data points (Q, W) obtained numerically by means of (32) for increasing flow depths in the considered cross-section surveys. The reproduced characteristics are obtained by fitting the calculated points (Q, W) to the power function model (1). Logarithms are introduced to solve the problem as an OLS linear regression, so that the scaling coefficient a' and the exponent b' are obtained from the intercept and the coefficient, respectively, of the straight line

$$\log W = \log a' + b' \log Q. \tag{33}$$

For section 149 (where $k_S = 18.92$ m$^{1/3}$ s^{-1} and $S_o = 0.0025$), $a' = 7.49$ m$^{0.22}$ s$^{0.26}$ and $b' = 0.26$, while for section 22 (where $k_S = 24.59$ m$^{1/3}$ s^{-1} and $S_o = 0.0018$), $a' = 13.39$ m$^{0.25}$ s$^{0.25}$ and $b' = 0.25$, in consequence of different roughness, slope, and shape of the two cross sections. The goodness-of-fit is expressed through the coefficients of determination r^2, equal to 0.98 and 0.90 for the two considered regressions, respectively.

In order to determine the downstream variability for the considered characteristics, the at-a-station scaling coefficients and exponents for all 87 cross sections are plotted against the reduced upstream drainage area (A/A_o), A_o being the catchment area (Figure 6). With reference to the water-surface width W, the downstream variability of the at-a-station estimates of b' (data set (DS) in Figure 6a) are fitted to a straight line (merit function (MF) in Figure 6a) against (A/A_o) to test the possibility of taking b' constant throughout the considered drainage system, as assumed in the fluvial relationship (1) on which the proposed formulation is based. An OLS linear regression is performed, and both punctual estimates and 0.95 probability confidence intervals for the regression line coefficient are calculated on the basis of the assumption that the residuals between fitted data and regression function are normally distributed (this implies also that the coefficient of the regression line is normally distributed (this implies also that the coefficient of the regression line is normally distributed, being a linear function of normal random variables). For our sample of 87 data points the value of the Student's t distribution with 85 degrees of freedom corresponding to the cumulative probability 0.975, namely 1.992, is used to calculate the limits of the 0.95 probability confidence interval for the regression line coefficient. Such limits are obtained from the punctual estimate (−0.07) by subtracting and adding the standard deviation (4.03×10^{-2}) multiplied by 1.992, respectively, yielding (−0.15, 0.01) (Table 1). The obtained punctual estimate of the linear regression coefficient and its confidence interval provide a measure of the reliability of assuming b' as a constant throughout the drainage system. Note that the value 0.00 is included in the obtained confidence interval, and this ensures that the null hypothesis "b' = constant" is verified at the significance level 0.05. If the hypothesis b' = constant can be accepted, the mean value

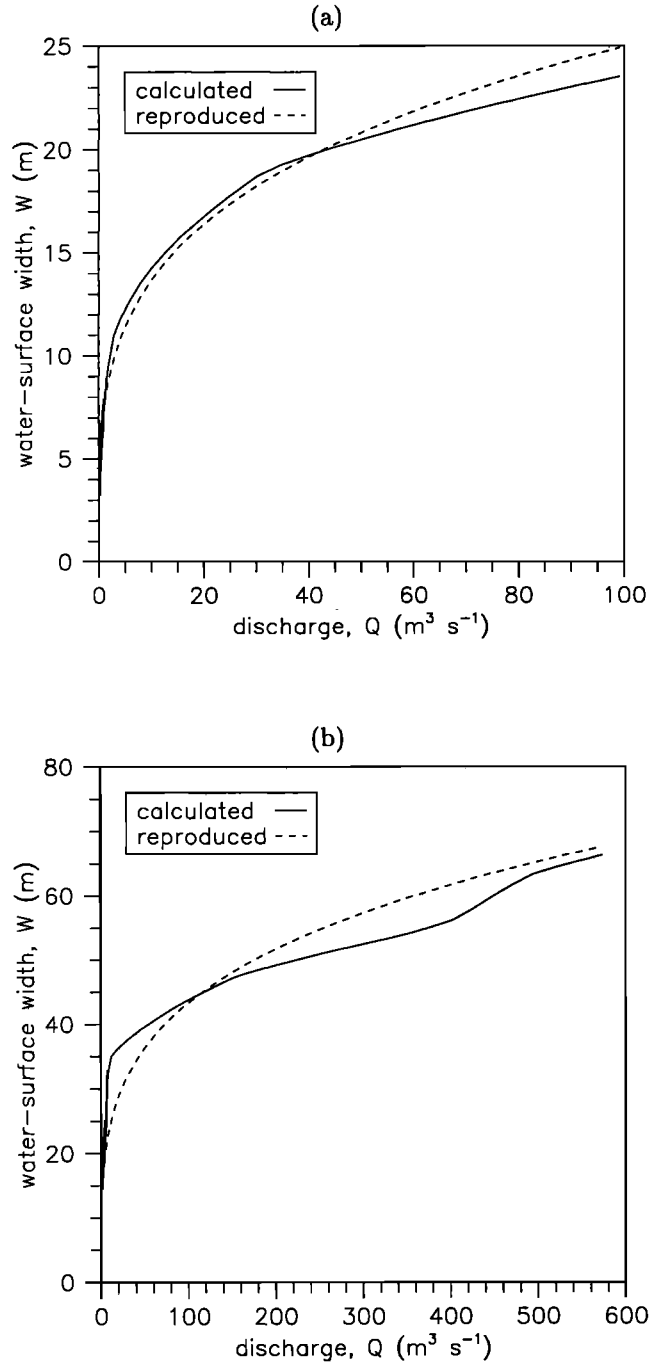

Figure 5. Calculated and reproduced at-a-station width-discharge relationships for the two surveyed cross sections of Figure 4: (a) section 149 and (b) section 22.

$$\langle b' \rangle = \frac{1}{N_s} \sum_{i=1}^{N_s} b'_i, \tag{34}$$

where N_s is the number of surveyed cross sections considered, can be assumed as representative of the entire drainage network, and its 0.95 probability confidence interval can be estimated to provide a measure of the reliability of the obtained value. In our case the mean value for b' results 0.26 and the relative confidence interval, (0.08, 0.44), is obtained from the mean value by subtracting and adding the standard deviation (9.13×10^{-2}) multiplied by the value of the Student's t distri-

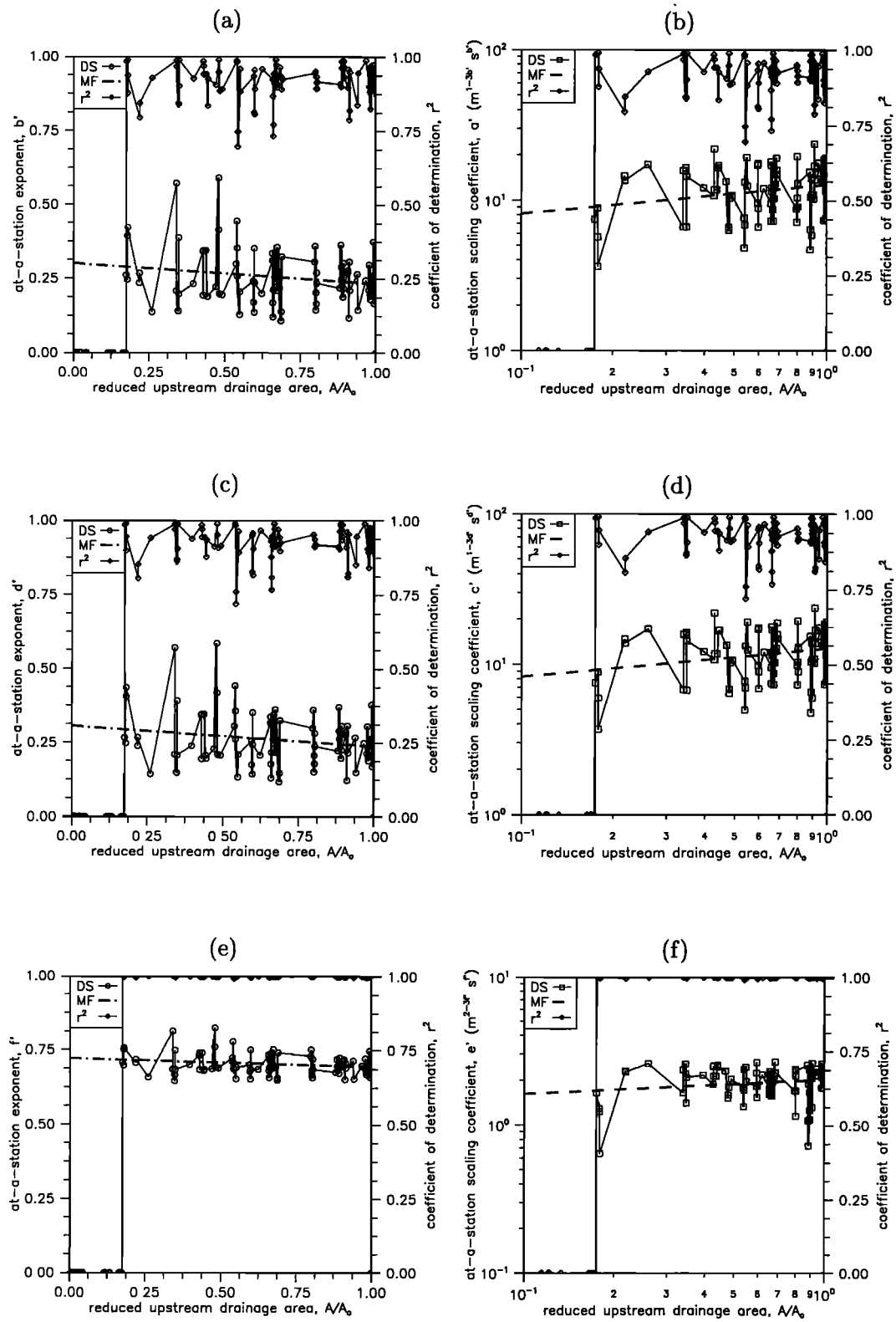

Figure 6. Downstream variability of exponents and scaling coefficients as obtained by plotting at-a-station OLS regression estimates (data sets (DSs)) and by fitting these estimates to a straight line (merit functions (MFs)) (Table 1). Coefficients of determination refer to the at-a-station linear regressions.

bution with 86 degrees of freedom corresponding to the cumulative probability 0.975, namely 1.991 (Table 2). If the assumption b' = constant is not verified for a given drainage system, the illustrated procedure, as presently formulated, is not applicable.

Estimates of the downstream parameters $W_{r\,o}$ and b'' introduced in section 2.1 are obtained by considering (9) in the logarithmic form

$$\log {}^{\omega}W = \log (W_{r\,o} Q_{r\,o}^{-b'}) + (b'' - b') \log (A/A_o), \qquad (35)$$

W being equal to the estimated at-a-station coefficient a' for each considered cross section. Points $((A/A_o), a')$ obtained from the at-a-station regressions (DS in Figure 6b) are fitted in a logarithmic plot to a straight line (MF in Figure 6b) of intercept $(W_{r\,o}Q_{r\,o}^{-b'})$ and coefficient $(b'' - b')$. The value of the Student's t distribution with 85 degrees of freedom corresponding to the cumulative probability 0.975, namely 1.992, is used to calculate the limits of the 0.95 probability confidence interval for OLS regression intercept and coefficient. Since $Q_{r\,o}$ is set equal to 1 $m^3\ s^{-1}$, the obtained intercept is $W_{r\,o} = 12.73$ m with confidence interval (11.27, 14.38) m, whereas the coefficient $(b'' - b')$ is 0.20 with confidence interval (0.02, 0.38) (Table 1). The obtained estimates for $W_{r\,o}$ and $(b'' - b')$ are also summarized in Table 2 along with punctual estimate and confidence interval for b'', 0.46 and (0.10, 0.82) respectively, which are calculated by propagating punctual estimates and confidence intervals of b' and $(b'' - b')$ through the addition.

The procedure of parameterization illustrated with reference to the water-surface width W is also applied to reproduce all the at-a-station and downstream characteristics for wetted perimeter P (Figures 6c and 6d) and flow area Ω (Figures 6e and 6f). The obtained OLS regressions intercepts and coefficients are reported in Table 1, whereas the channel geometry parameters are summarized in Table 2. All the estimated parameters for the Sieve catchment hydraulic geometry are in the range of those obtained in more detailed field inspections [e.g., *Leopold and Maddock*, 1953; *Pilgrim*, 1977]. Note that the estimated parameters for the water-surface width ($W_{r\,o}$, b', b'') do not significantly differ from those estimated for the wetted perimeter ($P_{r\,o}$, d', d'') in consequence of the wideness of the considered natural cross sections. Under these circumstances ($W_{r\,o} \simeq P_{r\,o}$, $b' \simeq d'$, and $b'' \simeq d''$) the effects of the dynamic variations in channel geometry in distributed, DEM-based flood routing models can be thought of as being described by routing surface runoff over a network composed of wide rectangular channels whose width W is allowed to vary dynamically with discharge according to (8) and (9). This follows from the fact that the Manning-Gauckler-Strickler friction equation for wide rectangular channels exhibits the same form of the general equation (26) with $W(Q)$ in place of $P(Q)$. Parameters ($\Omega_{r\,o}$, f', f'') of the flow area relationship (16) are estimated to synthesize the at-a-station and downstream variability of Ω with Q provided by the resistance law (32). These parameters will be used in section 3.2 to obtain the law of variability in space and time for the Froude number, which expresses the possible influence of downstream disturbances on flow propagation.

Table 1. Estimated OLS Regression Intercepts and Coefficients of the Sieve Channel Geometry Parameters

IV	DV	Intercept	Coefficient
A/A_o	b'	0.30 (0.24, 0.36)	−0.07 (−0.15, 0.01)
A/A_o	a', $m^{1-3b'}\ s^{b'}$	12.73 (11.27, 14.38)	0.20 (0.02, 0.38)
A/A_o	d'	0.31 (0.25, 0.37)	−0.07 (−0.15, 0.01)
A/A_o	c', $m^{1-3d'}\ s^{d'}$	12.76 (11.32, 14.37)	0.19 (0.01, 0.37)
A/A_o	f'	0.72 (0.70, 0.74)	−0.03 (−0.06, 0.00)
A/A_o	e', $m^{2-3f'}\ s^{f'}$	2.05 (1.88, 2.23)	0.10 (−0.03, 0.23)

IV, independent variable; DV, dependent variable. Values in parentheses indicate the lower and upper limits of the 0.95 probability confidence interval.

Table 2. Estimated Parameters of the Sieve Channel Geometry

Parameter	Estimate
b'	0.26 (0.08, 0.44)
$W_{r\,o}$, m	12.73* (11.27, 14.38)
$b'' - b'$	0.20 (0.02, 0.38)
b''	0.46 (0.10, 0.82)
d'	0.26 (0.08, 0.44)
$P_{r\,o}$, m	12.76* (11.32, 14.37)
$d'' - d'$	0.19 (0.01, 0.37)
d''	0.45 (0.09, 0.81)
f'	0.70 (0.63, 0.77)
$\Omega_{r\,o}$, m^2	2.05* (1.88, 2.23)
$f'' - f'$	0.10 (−0.03, 0.23)
f''	0.80 (0.60, 1.00)

Values in parentheses indicate the lower and the upper limits of the 0.95 probability confidence intervals.
*Having assumed $Q_{r\,o} = 1\ m^3\ s^{-1}$.

3.2. Routing Surface Runoff

The catchment model was run over several observed flood events among which the December 1979 event is used in the following analysis. The selection of the December 1979 event is motivated by the fact that the corresponding hydrograph appears to be well reproduced (with respect to other hydrographs) in the initial part of the rising limb, and this outcome is used in the context of the present study to justify the assumption that surface runoff hydrograph timing is mainly related to network routing dynamics rather than to runoff production mechanisms (Figure 7). The impact of the channel geometry estimated in section 3.1 on network routing is assessed by comparing the simulated catchment response at two different levels of conceptualization of the channel system. At the first level the case in which the channel network is assumed to be composed of wide rectangular channels of variable width in a downstream direction but not at a given station with discharge ($b' = 0$ in (8)) is considered (the static channel network (SCN) case). At the second level the case in which the

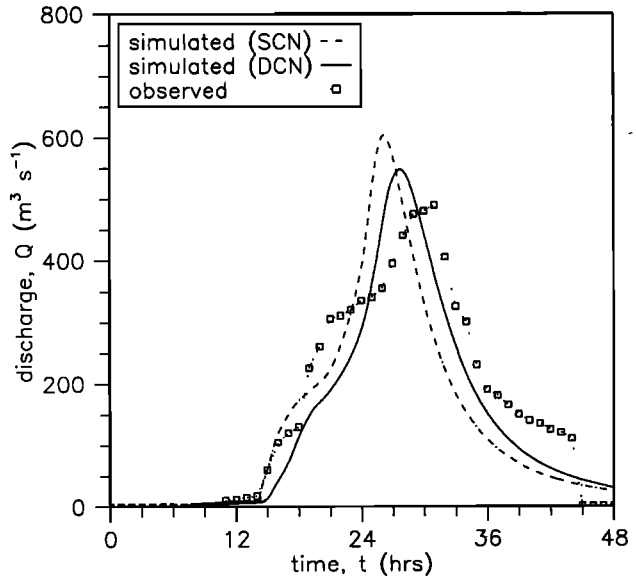

Figure 7. Comparison between simulated and observed outlet hydrographs for the December 1979 Sieve catchment event.

Table 3. Parameterization of the Sieve Catchment Drainage System for Flow Simulations

Parameter	Rill Flow	Channel Flow	
		Static Description	Dynamic Description
$Q_{r\,o}$, $m^3\ s^{-1}$	657.63*	1.00	1.00
$W_{r\,o}$, m	989.10†	25.00	12.73
b'	0.26	0.00	0.26
b''	0.46	0.46	0.46
k_S,‡ $m^{1/3}\ s^{-1}$	0.70	16.00–25.00	16.00–25.00

*Value set so as to obtain $Q_r = 1.00\ m^3\ s^{-1}$ for $A = A_*$ (by means of (7) with $A_* = 1.28\ km^2$ and $A_o = 841.76\ km^2$).

†Value set so as to obtain $W_r = 50.00$ m for $A = A_*$ (by means of (4) with $Q_r = 1.00\ m^3\ s^{-1}$).

‡Here $k_S = 1/n$, n being the Manning roughness, $m^{-1/3}$ s.

channel network is assumed to be composed of wide rectangular channels of width variable both in a downstream direction and at a given station ($b' = 0.26$ in (8)) is considered (the dynamic channel network (DCN) case), so as to reproduce the estimated channel geometry (see the last paragraph of section 3.1).

As shown in Table 3, in the static case $b' = 0$, $b'' = 0.46$ as obtained in section 3.1, and the channel width at the catchment outlet $W_{r\,o}$ is assumed to be 25.00 m. This value is approximately the water-surface width corresponding to the mean annual discharge $Q = 13.41\ m^3\ s^{-1}$ at the Sieve catchment outlet, which is assumed in the context of the present study as a discharge with channel-forming significance (channel-forming discharge) [*Knighton*, 1987]. As obtained from (8) and (9), in the static case water-surface width W is scaled upstream from the outlet value $W_{r\,o} = 25.00$ m ($Q_{r\,o}$ has no effects for $b' = 0$) with the reduced upstream drainage area (A/A_o) to the exponent $b'' = 0.46$ (Table 4) but it is not allowed to vary at a given station dynamically with discharge Q, b' being equal to zero. In the dynamic case the effects of the dynamic variations in the Sieve channel geometry on flow propagation are reproduced using values $W_{r\,o} = 12.73$ m, $b' = 0.26$, and $b'' = 0.46$ estimated in section 3.1 in the routing model developed in section 2.2 with $\mathcal{P} \simeq \mathcal{W}$ and $d' \simeq b'$. As obtained from (8) and (9), in the dynamic case water-surface width W is scaled upstream from the outlet value $W_{r\,o} = 12.73$ m (corresponding to $Q_{r\,o} = 1\ m^3\ s^{-1}$) with the reduced upstream drainage area (A/A_o) to the exponent $b'' - b' = 0.20$ (Table 4), and it is allowed to vary at any given station dynamically with discharge Q to the exponent $b' = 0.26$. The Gauckler-Strickler roughness coefficient k_S for channel flow is assumed to be variable upstream from 25.00 $m^{1/3}\ s^{-1}$ to 16.00 $m^{1/3}\ s^{-1}$ on the basis of data reported in the literature [e.g., *Bathurst*, 1993]. No field measurements are available to characterize rill flow dynamics, and thus rill geometry and roughness are empirically evaluated on the basis of studies reported in the literature [e.g., *Newson and Harrison*, 1978; *Emmett*, 1978; *Kouwen and Li*, 1980; *Bathurst*, 1986]. The structural parameter $Q_{r\,o}$ is set equal to the value 657.63 $m^3\ s^{-1}$ so as to obtain $Q_r = 1.00\ m^3\ s^{-1}$ for $A = A_*$ by means of (7) with $A_* = 1.28\ km^2$ and $A_o = 841.76\ km^2$, and $W_{r\,o}$ is set equal to 989.10 m so as to obtain $W_r = 50.00$ m for $A = A_*$ by means of (4) with $Q_r = 1.00\ m^3\ s^{-1}$. The Gauckler-Strickler roughness coefficient k_S for rill flow is assumed to be 0.70 $m^{1/3}\ s^{-1}$.

Simulated and observed outlet hydrographs for the December 1979 flood event are plotted in Figure 7. The hydrograph peak simulated in the dynamic channel network case is lagged and reduced with respect to the hydrograph peak simulated in the static channel network case. The lag between the two simulated peaks is approximately equal to 1.5 hours (~15% of the rising limb duration), and the peak discharge is reduced by about 56 $m^3\ s^{-1}$ (~10%), allowing a significant improvement in the reproduction of the observed catchment response. In Figure 8 the catchment response is calibrated using b' as a fitting parameter. Hydrograph peak and time to peak are well reproduced for $b' = 0.38$, which may indicate a stronger influence of storage in the Sieve catchment drainage network than is represented by the value $b' = 0.26$, obtained consid-

Table 4. Characteristics of the Main Stream of the Sieve Catchment With Reference to the Spatial Discretization Shown in Figure 9

CN	X, m	Y, m	i	j	k	s, km	CSN	A, km^2	$\mathcal{W}$(SCN), m	$\mathcal{W}$(DCN), $m^{0.22}\ s^{0.26}$
···	1674198.0	4870648.5	1	54	1	0.00	···	0.00	0.00	0.00
A	1677798.0	4872248.5	10	58	11	4.83	···	20.64	4.54	6.06
B	1681398.0	4871848.5	19	57	21	9.16	···	102.24	9.48	8.35
···	1684598.0	4870648.5	27	54	29	12.77	149	146.56	11.19	8.97
C	1685779.0	4871131.0	29	55	31	13.74	146	150.08	11.31	9.02
D	1689803.9	4869543.5	39	51	41	18.65	125	293.12	15.39	10.31
E	1694051.4	4867337.0	49	47	51	23.65	112	402.72	17.81	10.98
F	1698246.5	4867184.0	59	45	61	28.22	96	500.32	19.68	11.47
G	1701009.4	4866003.0	67	43	71	32.56	84	556.48	20.67	11.72
H	1702658.1	4862682.5	72	34	81	37.22	70	670.56	22.52	12.16
I	1702398.0	4859064.0	71	25	91	41.88	58	745.76	23.65	12.43
L	1699551.8	4855698.0	65	17	101	46.88	31	789.76	24.28	12.57
···	1697798.0	4852248.5	60	8	110	51.30	22	830.08	24.84	12.69
M	1698360.5	4851885.0	61	7	111	51.87	21	834.88	24.91	12.71
N	1696598.0	4849448.5	57	1	118	55.57	···	841.76	25.00	12.73

CN, cell name; CSN, cross-section number. X and Y, UTM coordinate in the x direction and y direction, respectively; i, j, and k, DEM cell index in the x direction, in the y direction, and along the selected path, respectively; s, spatial coordinate along the selected path (positive downstream); A, upstream drainage area; $\mathcal{W}$(SCN) and $\mathcal{W}$(DCN), water-surface width scaling coefficient in the static channel network (SCN) and in the dynamic channel network (DCN) description, respectively.

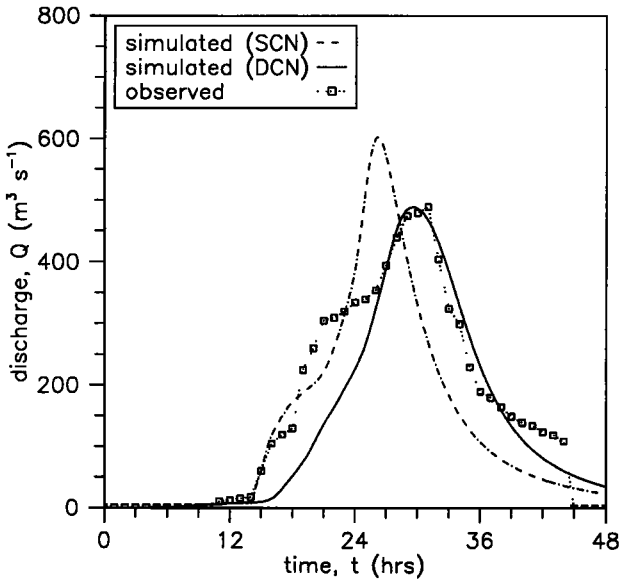

Figure 8. Comparison between simulated and observed outlet hydrographs for the December 1979 Sieve catchment event, where b' is used as a fitting parameter. The flood wave peak is well reproduced in magnitude and timing for $b' = 0.38$.

ering only macroscopic features of the cross-sectional shapes. This discrepancy could also be due to other model assumptions, such as that of constant channel roughness at any given station for variable flow depth.

The space-time variability of flow velocity $U = Q/\Omega$ in the drainage network is investigated by performing a "downstream" analysis of catchment dynamics along the path shown in Figure 9 and described in Table 4. The variations of flow discharge and velocity along the selected path in the static channel network case are shown in Figures 10a and 10b, respectively, whereas Figures 10c and 10d refer to the dynamic channel network case. Flow velocity is shown to vary little in space in spite of a significant variation in flow discharge, in agreement with published field data [e.g., *Carlston*, 1969; *Pilgrim*, 1977]. A significant variability in time of the velocity field during the flood event is also revealed. These results indicate that the assumption of velocities and travel times constant in space and time used in many procedures of hydrograph synthesis [e.g., *Rodriguez-Iturbe and Valdes*, 1979; *Cabral et al.*, 1990] may be reasonable regarding the variability of velocity in space but it may be inadequate regarding the variability of velocity in time, during the flood event. In addition, it is important to note how flow velocities in the dynamic channel network case (Figure 10d) are significantly reduced with respect to those obtained in the static channel network case (Figure 10b), in spite of relatively minor reductions of flow discharge (Figures 10a and 10c). The control of stream channel geometry on simulated catchment dynamics may therefore provide, at least in part, a physical explanation of the low values of overland flow and streamflow velocities, namely $U_o = 0.16$ m s^{-1} and $U_s = 1.67$ m s^{-1}, obtained by *Cabral et al.* [1990] by routing surface runoff through a DEM-based drainage network of the Sieve catchment and using U_o and U_s as fitting parameters.

The results obtained indicate the importance of incorporating the essential features of the stream channel geometry into the distributed modeling of catchment dynamics. The major shortcoming of the developed formulation is the inability of the routing scheme to handle downstream disturbances. The influence of downstream disturbances on flow propagation can be expressed in terms of Froude number

$$Fr = U/\sqrt{gY_m}, \tag{36}$$

where $U = Q/\Omega$ is the mean flow velocity and $Y_m = \Omega/W$ is the hydraulic depth (mean flow depth), which provides a measure of the influence of the inertial forces with respect to gravitational forces. If $Fr = 1$, the flow is critical and inertial and gravitational forces are in equilibrium. If $Fr < 1$, the flow is subcritical and the gravitational forces are dominant. If $Fr > 1$, the flow is supercritical and the inertial forces are dominant. Incorporating (8), (9), and (16) into (36) and using the parameter estimates reported in Table 2 yields

$$Fr = 0.39(A/A_o)^{-0.05}Q^{0.08}, \tag{37}$$

which reveals that (for realistic values of (A/A_o) and Q) the flow in the Sieve catchment network is generally subcritical and thus influenced by downstream disturbances. Several criteria were proposed for determining when the backwater effects can be neglected [e.g., *Miller*, 1984; *Ponce et al.*, 1978], but there is not a single, universal criterion for making this decision. An assessment of the influence of downstream disturbances on flood propagation must therefore be carried out for the considered drainage system for an appropriate application of the

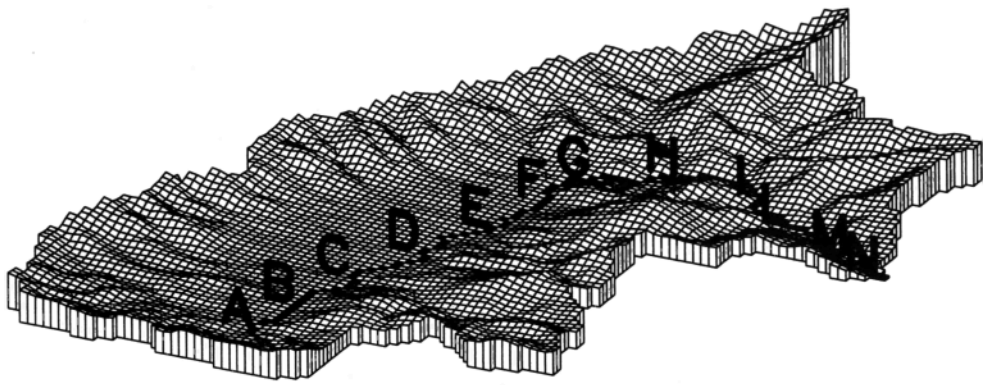

Figure 9. A 400 m × 400 m DEM of the Sieve catchment showing the path selected for the "downstream" analysis of the December 1979 flood event (Table 4).

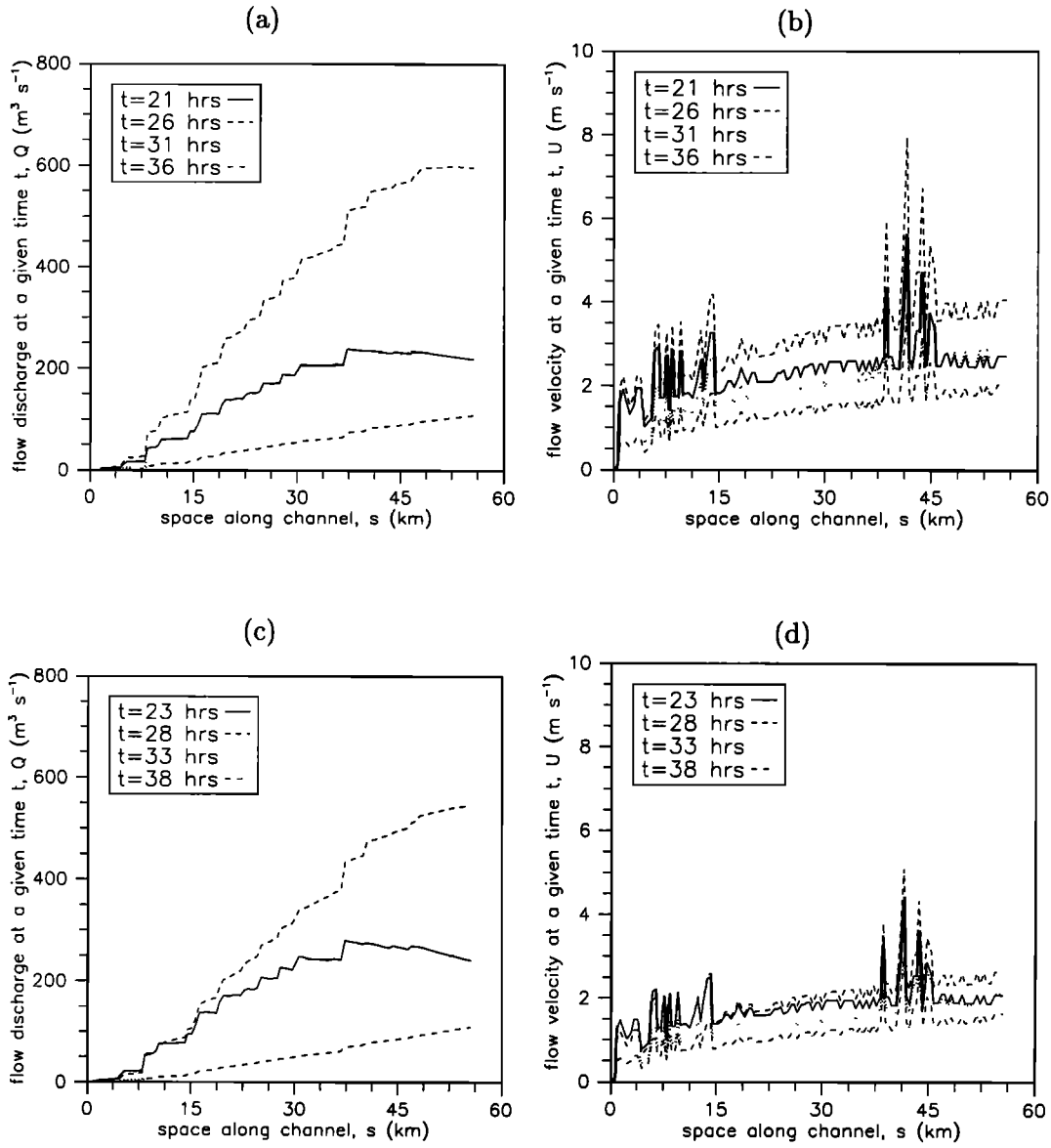

Figure 10. Surface runoff discharge and velocity along the path shown in Figure 9 for different instants in time of the December 1979 Sieve catchment event (Figure 7): (a), (b) static channel network case and (c), (d) dynamic channel network case.

routing scheme. However, it is remarked here how the parameterization of the stream channel geometry developed in the present study (equations (28) and (29)) has general validity and thus, if necessary, can be incorporated into more complex discretizations of the diffusion wave equation where backwater effects are reproduced [e.g., *Julien et al.*, 1995; *Moussa and Bocquillon*, 1996].

4. Summary and Conclusions

Water-surface width and wetted perimeter fluvial relationships were incorporated into a diffusion wave routing scheme to provide an efficient parameterization of channel geometry in the distributed modeling of catchment dynamics. The developed formulation was applied to the 840-km^2 Sieve catchment (Central Italian Apennines) to describe both the hillslope rill and network channel surface flow processes during flooding conditions. Insights were sought into the impact of the distributed storages related to the locally varying network channel shape on surface runoff propagation. Since no distributed flow measurements were available, uniform flow characteristics for a set of 87 surveyed cross sections along the catchment mainstream were calculated on the basis of the Manning-Gauckler-Strickler friction equation for composite sections and the obtained results were used as standards to estimate the at-a-station and downstream channel geometry parameters. OLS regressions were carried out, and both punctual estimates and limits of the 0.95 confidence intervals were calculated in order to provide a measure of the reliability of the adopted parameterization. The obtained estimates were found to be in the range of those obtained from more detailed field inspections [e.g., *Leopold and Maddock*, 1953; *Pilgrim*, 1977].

Wetted perimeter parameters ($P_{r\,o}$, d', d'') were found not to significantly differ from the corresponding water-surface width parameters ($W_{r\,o}$, b', b''), as generally happens for

natural channels. Under these conditions, from the obtained expressions for flow celerity c_k (equation (28)) and hydraulic diffusivity D_h (equation (29)), it is revealed how the hydraulic effects of channel geometry on the diffusion wave flow propagation can be reproduced by routing surface runoff on a network composed of wide rectangular channels with dynamically variable width. This ascertainment was used to assess the impact of the estimated channel geometry on catchment dynamics. Local contributions to infiltration excess runoff were routed through a DEM-based drainage network for which channel geometry was described at two different levels of conceptualization, the static channel network case and the dynamic channel network case.

The December 1979 flood event was selected among other events since the corresponding outlet hydrograph appeared to be well reproduced in the initial part of the rising limb, and this was used to justify the assumption that the hydrograph timing can mainly be related to channel network dynamics rather than to runoff production mechanisms. The outlet hydrograph obtained by routing surface runoff over the dynamic channel network was shown to improve significantly the reproduction of both observed peak discharge and time to peak with respect to the hydrograph obtained in the static channel network case. A greater value of the at-a-station width exponent ($b' = 0.38$) with respect to the obtained estimate ($b' = 0.26$) was found to be required to fit simulated and observed hydrograph peak and time to peak. This discrepancy may indicate a stronger influence of storage in the Sieve drainage system than is represented by the value $b' = 0.26$, obtained considering only the macroscopic features of cross-sectional shapes. It could also be due to other model assumptions, such as that of constant channel roughness at a given station for variable stage. From a "downstream" analysis of the simulated flood event, the variation of flow velocity along the drainage network for a given instant in time was found to be slight with respect to the variation of flow discharge, in agreement with published field data. A significant dynamics of the velocity field during the flood phenomenon was revealed, in disagreement with the assumption of stationary velocity made in many procedures for flood hydrograph synthesis.

Shortcomings of the developed formulation are that (1) it cannot handle downstream disturbances, and thus caution must be exercised in upscaling the model application from steep mountain catchments to broad low-gradient valleys; (2) the use of spatially varying hydraulic geometry will be useful for flows close to, but not exceeding, bankfull, and thus the hydraulic geometry characterization will not, as presently formulated, be useful for overbank flooding conditions; and (3) hillslope rill and network channel roughness are allowed to vary in a downstream direction but not at a given station, dynamically with discharge. Despite these limitations, the simulation results obtained thus far are encouraging. The combined use of DEM-derived drainage network structure, scaling concepts for hydraulic geometry of channels, and diffusion wave equations for both hillslope rill and network channel flows can help in investigating nonlinear dynamics of basin response to storm rainfall, where basin topography plays an important role. Although simultaneous measurements of stream channel geometry and flow characteristics would be required to obtain a robust parameterization of the hydraulic geometry of a natural drainage system (especially for hillslope areas), the estimation procedure illustrated in the present study seems to be a potentially useful tool for those cases in which only surveyed cross sections are available. In addition, it is important to remark how the reliability of the proposed estimation procedure can be verified during its various steps by means of the confidence intervals of the OLS regression estimates. The results obtained from a "downstream" analysis of the velocity field indicate that the stream characteristics related to the locally varying cross-section shape may have a strong control on flow velocities, and thus they should be monitored and synthesized for a comprehensive description of the distributed catchment dynamics. This may be especially relevant in the simulation of those catchment processes for which detailed descriptions of flow velocity and hydraulic geometry are required, such as the transport of sediments and pollutants.

Appendix: Characteristics of Flow in Natural Channels

The Manning-Gauckler-Strickler friction equation for generally shaped cross sections (26) can be put in the implicit form

$$F(Q, \Omega) = 0, \tag{A1}$$

where $F(Q, \Omega) = Q - k_S S_f^{1/2} P(Q)^{-2/3} \Omega^{5/3}$, so that the kinematic wave celerity $c_k = dQ/d\Omega$ in (23) can be obtained by applying Dini's theorem as

$$\frac{dQ}{d\Omega} = -\frac{\partial F}{\partial \Omega} \Big/ \frac{\partial F}{\partial Q}. \tag{A2}$$

One can obtain

$$\frac{dQ}{d\Omega} = \frac{5/3 k_S S_f^{1/2} P(Q)^{-2/3} \Omega^{2/3}}{1 + \frac{2}{3} k_S S_f^{1/2} \Omega^{5/3} P(Q)^{-5/3} \dfrac{dP(Q)}{dQ}}. \tag{A3}$$

Equation (28) is obtained by incorporating (12) into (A3), where S_f is ultimately assumed equal to the channel bed slope S_o on the basis of the kinematic flow assumption.

The hydraulic diffusivity D_h in (25) is derived from the continuity equation and a simplified momentum equation

$$\frac{\partial \Omega}{\partial t} + \frac{\partial Q}{\partial s} = q_L, \tag{A4}$$

$$\frac{\partial (Y \cos \beta)}{\partial s} = S_o - S_f, \tag{A5}$$

where s and t are the spatial and temporal coordinates, respectively; Ω is the flow area; Q is the discharge; q_L is the lateral inflow; Y is the flow depth; β is the channel bed inclination angle; $S_o = \sin \beta$ is the channel bed slope; and S_f is the friction slope [*Hayami*, 1951]. Since $\partial \Omega/\partial t = d\Omega/dY \, \partial Y/\partial t$, (A4) can be written in the form

$$W \frac{\partial Y}{\partial t} + \frac{\partial Q}{\partial s} = q_L, \tag{A6}$$

$W = d\Omega/dY$ being the water-surface width. Equations (A5) and (A6) can be combined into a single equation by taking the derivative of the first with respect to t and of the second with respect to s in order to eliminate the mixed derivative $\partial^2 Y/(\partial s \partial t)$. Incorporating the formula

$$\frac{\partial S_f}{\partial t} = \frac{\partial S_f}{\partial Q} \frac{\partial Q}{\partial t} + \frac{\partial S_f}{\partial Y} \frac{\partial Y}{\partial t} \tag{A7}$$

and the expression of $\partial Y/\partial t$ given by (A6) into the obtained combination equation, for $\partial q_L/\partial s = 0$ and $\partial W/\partial s\ \partial Y/\partial t = 0$, yields

$$\frac{\partial^2 Q}{\partial s^2} = \frac{1}{D_h}\left[\frac{\partial Q}{\partial t} - c_k\left(q_L - \frac{\partial Q}{\partial s}\right)\right], \tag{A8}$$

(which corresponds to (25)), where

$$c_k = -\frac{\partial S_f}{\partial \Omega}\Big/\frac{\partial S_f}{\partial Q} \tag{A9}$$

is the kinematic celerity as given by (A2) and

$$D_h = 1\Big/\left(\frac{W}{\cos\beta}\frac{\partial S_f}{\partial Q}\right). \tag{A10}$$

Taking the derivative of (26) solved for S_f, one can obtain

$$D_h = \frac{Q\cos\beta}{2WS_f\left[1 + \frac{2}{3}\frac{Q}{P(Q)}\frac{dP(Q)}{dQ}\right]}. \tag{A11}$$

Equation (29) is obtained by incorporating (8) and (12) into (A11), where S_f is ultimately assumed equal to the channel bed slope S_o on the basis of the kinematic flow assumption.

Acknowledgments. This research was jointly supported by the Gruppo Nazionale per la Difesa dalle Catastrofi Idrogeologiche, contribution 97.00061.PF42, and by the European Community, through the grants ENV4-CT97-0552 (MAP-RAPHAEL project) and ENV4-CT97-0529 (FRAMEWORK project). Giuseppe Batini (Servizio Idrografico e Mareografico Nazionale, Roma, Italy, General Director) is gratefully acknowledged for providing land surveys of the Sieve catchment necessary for the present study. The authors thank Claudio Paniconi (CRS4, Cagliari, Italy), Alan D. Howard (University of Virginia, Charlottesville), and the anonymous reviewers for comments that led to improvements in the manuscript.

References

Band, L. E., Topographic partition of watersheds with digital elevation models, *Water Resour. Res.*, *22*(1), 15–24, 1986.

Bathurst, J. C., Physically-based distributed modelling of an upland catchment using the Système Hydrologique Européen, *J. Hydrol.*, *87*, 79–102, 1986.

Bathurst, J. C., Flow resistance through the channel network, in *Channel Network Hydrology*, edited by K. Beven and M. J. Kirkby, pp. 69–98, John Wiley, New York, 1993.

Beven, K., and P. E. O'Connell, On the role of distributed models in hydrology, *Rep. 81*, Inst. of Hydrol., Wallingford, U. K., 1982.

Beven, K., and E. F. Wood, Flow routing and the hydrological response of channel networks, in *Channel Network Hydrology*, edited by K. Beven and M. J. Kirkby, pp. 99–128, John Wiley, New York, 1993.

Blench, T., Regime theory for self-formed sediment bearing channels, *Trans. Am. Soc. Civ. Eng.*, *117*, 1–18, 1951.

Bras, R. L., *Hydrology: An Introduction to Hydrologic Science*, Addison-Wesley, Reading, Mass., 1990.

Cabral, M. C., R. L. Bras, D. Tarboton, and D. Entekhabi, A distributed, physically-based, rainfall-runoff model incorporating topography for real-time flood forecasting, *Rep. 332*, Ralph M. Parsons Lab., Dep. of Civ. Eng., Mass. Inst. of Technol., Cambridge, 1990.

Carlá, R., A. Carrara, and G. Federici, Generazione dei modelli digitali dei terreni ad alta precisione, *Publ. 0/87*, Univ. di Firenze, Dipartimento di Ing. Civ., Firenze, Italy, 1987.

Carlston, C. W., Downstream variations in the hydraulic geometry of streams: Special emphasis on mean velocity, *Am. J. Sci.*, *267*, 499–509, 1969.

Cunge, J. A., On the subject of a flood propagation computation method (Muskingum method), *J. Hydraul. Res.*, *7*(2), 205–230, 1969.

Dooge, J. C. I., A general theory of the unit hydrograph, *J. Geophys. Res.*, *64*(2), 241–256, 1959.

Emmett, W. W., Overland flow, in *Hillslope Hydrology*, edited by M. J. Kirkby, pp. 145–176, John Wiley, New York, 1978.

Hayami, S., On the propagation of flood waves, *Bull. Disaster Prev. Res. Inst., Kyoto J. Univ.*, *1*(1), 1–16, 1951.

Howard, A. D., Role of hypsometry and planform in basin hydrologic response, *Hydrol. Processes*, *4*, 373–385, 1990.

Howard, A. D., A detachment-limited model of drainage basin evolution, *Water Resour. Res.*, *30*(7), 2261–2285, 1994.

Julien, P. Y., B. Saghafian, and F. L. Ogden, Raster-based hydrologic modeling of spatially-varied surface runoff, *Water Resour. Bull.*, *31*(3), 523–536, 1995.

Kennedy, R. G., The prevention of silting in irrigation canals, *Proc. Inst. Civ. Eng.*, *119*, 281–290, 1895.

Kirkby, M. J., Tests of a random network model and its application to basin hydrology, *Earth Surf. Processes*, *1*, 197–212, 1976.

Knighton, A. D., River channel adjustment—The downstream dimension, in *River Channels: Environment and Process*, edited by K. S. Richards, pp. 95–128, Blackwell, Cambridge, Mass., 1987.

Kolberg, F. J., and A. D. Howard, Active channel geometry and discharge relations of U.S. Piedmont and Midwestern streams: The variable exponent model revisited, *Water Resour. Res.*, *31*(9), 2353–2365, 1995.

Kouwen, N., and R. M. Li, Biomechanics of vegetative channel linings, *J. Hydraul. Div. Am. Soc. Civ. Eng.*, *106*, 1085–1103, 1980.

Lacey, G., Stable channels in alluvium, *Proc, Inst. Civ. Eng.*, *229*, 259–384, 1929.

Lacey, G., Regime flow in incoherent alluvium, *Publ. 20*, Cent. Board Irrig., Simla, India, 1939.

Lane, E. W., A study of the shape of channels formed by natural streams flowing in erodible material, *Mo. River Dist. Sediment Ser., Rep. 9*, U.S. Army Eng. Div., Omaha, Neb., 1957.

Leopold, L. B., and T. Maddock Jr., The hydraulic geometry of stream channels and some physiographic implications, *U.S. Geol. Surv. Prof. Pap. 252*, 1953.

Leopold, L. B., M. G. Wolman, and J. P. Miller, *Fluvial Processes in Geomorphology*, W. H. Freeman, New York, 1964.

Li, R. M., V. M. Ponce, and D. B. Simons, Modeling rill density, *J. Irrig. Drain. Div. Am. Soc. Civ. Eng.*, *106*(1), 63–67, 1980.

Mark, M. D., Automated detection of drainage networks from digital elevation models, *Auto Carto*, *6*, 169–178, 1983.

Miller, J. E., Basic concepts of kinematic-wave models, *U.S. Geol. Surv. Prof. Pap. 1302*, 1984.

Minshall, R. E., Predicting storm runoff on small experimental watersheds, *J. Hydraul. Div. Am. Soc. Civ. Eng.*, *86*(8), 28–33, 1960.

Montgomery, D. R., and E. Foufoula-Georgiou, Channel network source representation using digital elevation models, *Water Resour. Res.*, *29*(12), 3925–3934, 1993.

Morris, D. G., and R. G. Heerdegen, Automatically derived catchment boundaries and channel networks and their hydrological applications, *Geomorphology*, *1*, 131–141, 1988.

Mosley, M. P., Semi-determinate hydraulic geometry of river channels, Suoth Island, New Zeland, *Earth Surf. Processes Landforms*, *6*, 127–137, 1981.

Moussa, R., and C. Bocquillon, Algorithms for solving the diffusive wave flood routing equation, *Hydrol. Processes*, *10*, 105–123, 1996.

Myers, W. R. C., Influence of geometry on discharge capacity of open channels, *J. Hydraul. Eng.*, *117*(5), 676–670, 1991.

Natural Environment Research Council, Flood studies report, *Flood Routing Stud. III*, Inst. of Hydrol., Wallingford, U. K., 1975.

Newson, M. D., and J. G. Harrison, Channel studies in the Plynlimon experimental catchments, *Rep. 47*, Inst. of Hydrol., Wallingford, U. K., 1978.

Orlandini, S., and R. Rosso, Diffusion wave modeling of distributed catchment dynamics, *J. Hydraul. Eng.*, *1*(3), 103–113, 1996.

Orlandini, S., M. Mancini, C. Paniconi, and R. Rosso, Local contributions to infiltration excess runoff for a conceptual catchment scale model, *Water Resour. Res.*, *32*(7), 2003–2012, 1996.

Osterkamp, W. R., and E. R. Hedman, Variation of width and discharge for natural high-gradient stream channels, *Water Resour. Res.*, *13*(2), 256–258, 1977.

Park, C. C., Word-wide variations in hydraulic geometry exponents of stream channels: An analysis and some observations, *J. Hydrol.*, *33*, 133–146, 1977.

Pilgrim, D. H., Isochrones of travel time and distribution of flood

storage from a tracer study on a small watershed, *Water Resour. Res.*, *13*(3), 587–595, 1977.

Ponce, V. M., Diffusion wave modeling of catchment dynamics, *J. Hydraul. Eng.*, *112*(8), 716–727, 1986.

Ponce, V. M., and V. Yevjevich, Muskingum-Cunge method with variable parameters, *J. Hydraul. Div. Am. Soc. Civ. Eng.*, *104*(12), 1663–1667, 1978.

Ponce, V. M., R. M. Li, and D. B. Simons, Applicability of kinematic and diffusion models, *J. Hydraul. Div. Am. Soc. Civ. Eng.*, *104*(3), 353–360, 1978.

Rhoads, B. L., A continuously varying parameter model of downstream hydraulic geometry, *Water Resour. Res.*, *27*(8), 1865–1872, 1991.

Rodriguez-Iturbe, I., and J. B. Valdes, The geomorphologic structure of hydrologic response, *Water Resour. Res.*, *15*(6), 1409–1420, 1979.

Sherman, L. K., The relation of runoff to size and character of drainage basins, *Eos Trans. AGU*, *13*, 332–339, 1932.

Smith, T. R., C. Zhan, and P. Gao, A knowledge-based, two-step procedure for extracting channel networks from noisy DEM data, *Comput. Geosci.*, *16*, 777–786, 1990.

Wooding, R. A., A hydraulic model for the catchment-stream problem, I, Kinematic wave theory, *J. Hydrol.*, *3*, 254–267, 1965a.

Wooding, R. A., A hydraulic model for the catchment-stream problem, II, Numerical solutions, *J. Hydrol.*, *3*, 268–282, 1965b.

Wooding, R. A., A hydraulic model for the catchment-stream problem, III, Comparison with runoff observation, *J. Hydrol.*, *4*, 21–37, 1966.

S. Orlandini, Dipartimento di Ingegneria delle Strutture, dei Trasporti, delle Acque, del Rilevamento, del Territorio, Università degli Studi di Bologna, Viale Risorgimento 2, I-40136 Bologna, Italy. (e-mail: stefano@idraulica.ing.unibo.it)

R. Rosso, Dipartimento di Ingegneria Idraulica, Ambientale e del Rilevamento, Sezione Idraulica, Politecnico di Milano, Piazza Leonardo da Vinci 32, I-20133 Milano, Italy. (e-mail: rr@idra1.iar.polimi.it)

(Received October 29, 1997; revised January 20, 1998; accepted January 23, 1998.)